

Synthesis and Crystal Structure of 1, 10-Phenanthroline Bis(O, O' -di(2-phenylethyl) dithiophosphato) Nickel(II)

XIE Bin^{1,2}, ZOU Lirke^{1,2}, LAI Chuan³, HUANG Chun³, WANG Jun^{1,2}, XIANG Yang-guang³

(1 Institute of Functional Materials, Sichuan University of Science & Engineering Zigong 643000 China)

2 Key Laboratory of Green Chemistry of Sichuan Provincial University Zigong 643000 China

3 School of Material and Chemical Engineering Sichuan University of Science & Engineering Zigong 643000 China)

Abstract Reaction of complex $Ni[S_2P(OCH_2CH_2Ph)_2]_2$ with nitrogen base donor 1, 10-phenanthroline (phen) was carried out in petroleum ether and acetone solution to give green nitrogen base adduct 1, 10-phenanthroline bis(O, O' -di(2-phenylethyl)dithiophosphato) nickel(II), $Ni[S_2P(OCH_2CH_2Ph)_2]_2$ phen. The adduct was characterized by elemental analysis, UV-visible and IR spectra, thermal analysis and single-crystal X-ray diffraction. The crystal belongs to the monoclinic system, space group $P2_1/c$ with $a = 1.0987(9)$ nm, $b = 2.1432(9)$ nm, $c = 1.9025(5)$ nm, $\beta = 98.68(1)$ °, $V = 4.429(4)$ nm³, $Z = 4$. $D_c = 1.370$ Mg/m³, $F(000) = 1904$, $\mu = 0.743$ mm⁻¹, the final $R = 0.057$ and $wR = 0.1492$ for 3498 observed reflections ($I \geq 2\sigma(I)$). The Ni(II) atom adopts a distorted octahedral geometry with four sulfur atoms from two O, O' -di(2-phenylethyl)dithiophosphate ligands and two nitrogen atoms from a phen ligand. The N-S distances range from 0.2474(2) to 0.2505(17) nm, and the N-N distances are 0.2081(4) and 0.2090(5) nm. The overall structure of adduct consists of 1D chain-pair and 1D double-stranded helical chain, which formed from intermolecular π - π stacking C-H...O and C-H...S hydrogen-bonding interactions. They are further extended to 3D supramolecular network via C-H...O hydrogen-bonding interactions.

Key words O, O' -dialkyl dithiophosphate, nickel(II) adduct, synthesis, characterization, crystal structure

CLC number O614. 12

Document code A

Interest in the chemistry of metal complexes of O, O' -dialkyl dithiophosphates continues to grow due to extensively employed as antioxidant and antwear additives in rubber and lubricating oils^[1-2]. The complexes exhibit remarkable variety in their coordination geometries mono-, bi-, tetra-, or polynuclear and the O, O' -dialkyl dithiophosphate ligands act as monodentating chelating or bridging ligands in these complexes^[3-8]. Furthermore, the structures of the O, O' -dialkyl dithiophosphates and the categories of the metal can be modulated in an easily controlled manner to facilitate the individual application. The coordination system of nickel(II) is strongly dominated by mononuclearity with O, O' -dialkyl dithiophosphates ligands which is much different from

that of the readily-clustering metals cooper(I), zinc(II) and silver(I)^[6-8]. And these square planar four-coordinate nickel(II) complexes can be stabilized by the formation of five- and six-coordinate adducts with neutral donor ligands especially nitrogen bases e.g. ethylenediamine (en), pyridine (py), quinoline, 2, 2'-bipyridine (bipy) and 1, 10-phenanthroline (phen). These nitrogen bases are usually added to lubricating oils when the metal complexes of O, O' -dialkyl dithiophosphates serve as antioxidant additives of lubricating oils^[9-10], thus many metal adducts of O, O' -dialkyl dithiophosphates and nitrogen bases have been synthesized during the last two decades, but the alkyl groups of O, O' -dialkyl dithiophosphates in these ad-

ducts are very simple, such as Me, Et, n-Pr, i-Pr, n-Bu and cyclohexyl etc^[9-16]. However, only several molecular and crystal structures of nitrogen bases adducts of nickel(II) complexes with aryl dithiophosphates have been reported, where aryls are PhCH₂CH₂-^[17-18] and p-MeC₆H₄-^[19-20], so further studies on the influences of aromatic moiety to the coordinate behavior of nickel(II) are still necessary. Here we report the synthesis, characterization and crystal structure of 1, 10-phenanthroline adduct of bis(O, O'-di(2-phenylethyl) dithiophosphato) nickel(II), Ni[S₂P(OCH₂CH₂Ph)₂]₂• phen.

1 Experimental

1.1 Reagents and Physical Measurements

Melting point was determined on a WC-1 melting point apparatus without correction. Elemental analyses for carbon, hydrogen, nitrogen and sulfur were carried out on a Carlo-Erba 1106 elemental analyzer. The infrared spectrum was taken on a Nicolet MX-1 spectrometer by using KBr pellets. The ultraviolet-visible spectroscopy in CHCl₃ solution was obtained with a Jasco V-570 spectrophotometer. The thermal analysis was carried out with a Netzsch STA 409PC/PG in dry atmosphere at a heating rate of 10°C • m in⁻¹ from 35°C to 700°C. Single crystal X-ray diffraction analysis was carried out on an EnrafNonius CAD4 X-ray diffractometer.

All the chemicals were of analytical reagent grade and used directly without further purification. The compound (PhCH₂CH₂O)₂PS₂NH₂Et^[21] and the complex Ni[S₂P(OCH₂CH₂Ph)₂]₂^[22] was prepared according to the literature methods.

1.2 Synthesis

A solution of 0.198g (1mmol) 1, 10-phenanthroline (phen) in 10mL petroleum ether (90–120°C) was added dropwise to a hot solution of Ni[S₂P(OCH₂CH₂Ph)₂]₂ (0.356g 0.5mmol) in 25mL petroleum ether (90–120°C) and 25mL acetone under stirring. The solution was stirred at 40°C for 30 min, the green gelatinous precipitate was filtrated out and purified by column chromatography on silica gel G (V(acetone): V(petroleum ether) = 2: 1). The bright green solution was left to stand at room temperature after two weeks pale green prismatic crystals Ni[S₂P(OCH₂CH₂Ph)₂]₂• phen (1) suitable for X-ray analysis were obtained. Yield 45%, m.p. 150–152°C. Anal. calcd for C₄₄H₄₄N₂O₄P₂S₄Ni: C 57.85, H 4.85, N 3.07, S 14.04; Found (%): C 57.95, H 5.02, N 3.13, S 14.35. UV-vis(CHCl₃): λ_{max}: 382, 414, 661, 1122 nm; IR ν_{max}/cm⁻¹(KBr):

3027 w, 2953 w, 2885 w, 1626 m, 1604 m, 1496 s, 1453 m, 1422 s, 1378 m, 1341 w, 1086 m, 1057 s, 1028 s, 996 vs, 870 s, 850 s, 795 s, 727 s, 701 s, 670 s, 656 s, 601 s, 495 s.

1.3 Crystallographic Measurements and Structure Determination

A pale green prismatic crystal of adduct 1 with dimensions of 0.35mm × 0.20mm × 0.15mm was mounted on EnrafNonius CAD4 diffractometer equipped with a graphite monochromatized Mo Kα radiation (λ = 0.071073 nm) using the ω/2θ scan mode at 290(2) K. A total of 8025 reflections were measured in the range of 1.44 < θ < 25.01°, of which 7178 were independent with R_{int} = 0.0021 and 3498 were observed with I > 2σ(I). The structure was solved by direct methods using program SHELXS-97^[23] and refined by full-matrix least-squares with anisotropic thermal parameters for the non-hydrogen atoms on F² using program SHELXL-97^[23], spherical absorption correction was carried out by program WINGX (Version 1.70.01)^[24]. All hydrogen atoms were placed in the geometrically idealized positions with C-H = 0.093nm (aromatic), 0.099 nm (methylene) and refined as riding with U_{iso}(H) = 0.00110nm² (arylH) and 0.00129nm² (methyleneH).

Table 1 Crystal data and structure refinement of adduct 1

Empirical formula	C ₄₄ H ₄₄ N ₂ O ₄ P ₂ S ₄
Formal weight	913.70
Temperature K	290(2)
Volume /nm ³	4.429(4)
Crystal system	Monoclinic
Space group	P 2 ₁ /c
a /nm	1.0987(9)
b /nm	2.1432(9)
c /nm	1.9025(5)
β /°	98.68(4)
Z	4
ρ _{calcd} / (g•cm ⁻³)	1.370
μ /mm ⁻¹	0.743
F(000)	1904
Crystal size	0.35mm × 0.20mm × 0.15mm
h _{min} / h _{max}	-13/12
k _{min} / k _{max}	0/25
l _{min} / l _{max}	0/22
Reflections collected	8025
Independent reflections	7178(R _{int} = 0.0021)
Data/restraints/parameters	7178/2/516
Goodness-of-fit on F ²	1.067
Max and min transmission	0.8968 0.7811
Refinement method	Full-matrix least squares on F ²
R _p wR ₂ [I > 2σ(I)]	0.0577 0.1282
R _p wR ₂ (all data)	0.01492 0.1581
Largest diff peak and hole / e nm ⁻³	859/-478
w = 1/[σ ² (F _o ²) + (aP) ² + bP]	a = 0.0619 b = 0.0000
	P = (F _o ² + 2F _c ²)/3

Table 2 Selected bond lengths (nm) and bond angles (°) of adduct 1

N i(1)-N(1)	0. 2090(5)	S(2)-P(1)	0. 1972(3)
N i(1)-N(2)	0. 2081(4)	S(3)-P(2)	0. 1975(2)
N i(1)-S(1)	0. 2474(2)	S(4)-P(2)	0. 1978(2)
N i(1)-S(2)	0. 24839(18)	N(1)-C(1)	0. 1337(7)
N i(1)-S(3)	0. 25065(17)	N(1)-C(12)	0. 1351(7)
N i(1)-S(4)	0. 24970(18)	N(2)-C(10)	0. 1332(6)
S(1)-P(1)	0. 1974(2)	N(2)-C(11)	0. 1365(6)
N(1)-N i(1)-N(2)	79. 69(16)	S(1)-N i(1)-S(4)	90. 95(5)
N(1)-N i(1)-S(1)	170. 23(12)	P(2)-S(3)-N i(1)	82. 52(7)
N(2)-N i(1)-S(2)	95. 09(11)	P(2)-S(4)-N i(1)	82. 70(7)
N(2)-N i(1)-S(3)	167. 39(12)	N(2)-N i(1)-S(4)	97. 30(12)
N(2)-N i(1)-S(4)	90. 19(11)	N(2)-N i(1)-S(1)	95. 12(12)
P(1)-S(1)-N i(1)	84. 49(7)	S(2)-N i(1)-S(3)	94. 54(6)
P(1)-S(2)-N i(1)	84. 27(8)	S(2)-N i(1)-S(4)	170. 94(5)
N(1)-N i(1)-S(2)	90. 89(12)	S(3)-N i(1)-S(4)	81. 36(5)
N(1)-N i(1)-S(3)	92. 06(12)	S(2)-P(1)-S(1)	109. 81(10)
S(1)-N i(1)-S(2)	81. 27(5)	S(3)-P(2)-S(4)	111. 21(10)
S(1)-N i(1)-S(3)	94. 36(6)		

2 Results and Discussion

2.1 Crystal Structure

Single-crystal X-ray diffraction analysis reveals that the nitrogen base adduct **1** crystallizes in the monoclinic space group $P2_1/c$. The ORTEP view of **1** drawn at 30% probability displacement ellipsoids and the packing diagram in a unit are shown in Fig. 1, Fig. 2, Fig. 3, and Fig. 4 respectively. The crystal data and structure refinement for adduct **1** are given in Table 1. The selected bond lengths and angles of adduct **1** are given in Table 2. The hydrogen bond lengths and angles of adduct **1** are given in Table 3.

The space group $P2_1/c$ allows the two expected optical isomers to be present in the crystal lattice. Ni(II) ion adopts a distorted octahedral geometry with four sulfur atoms from two O, O' -di(2-phenyl ethyl) dithiophosphate ligands and two nitrogen atoms of phen ligand. In adduct **1**, the square planar structure of $\text{Ni}[\text{S}_2\text{P}(\text{OCH}_2\text{CH}_2\text{Ph})_2]_2^{[22]}$ has readily accommodated the bidentate phen ligand with two nitrogen atoms occupying *cis*-positions while maintaining the integrity of the two bidentate O, O' -di(2-phenyl ethyl) dithiophosphate ligands. Similar coordination geometry is seen in some six-coordinate analogues complex or adduct $\text{Ni}[\text{S}_2\text{P}(\text{OCH}_2\text{CH}_2\text{Ph})_2 \cdot \text{bipy}]^{[17]}$, $\text{Ni}[\text{S}_2\text{P}(\text{OC}_6\text{H}_4\text{M}-\text{o}-\text{p})]_2 \cdot \text{bipy}^{[19]}$, and $\text{Ni}[\text{S}_2\text{P}(\text{OC}_6\text{H}_4\text{M}-\text{e}-\text{p})]_2 \cdot \text{phen}^{[20]}$.

In adduct **1**, the $\text{Ni}-\text{S}$ distances range from 0. 2474 (2) to 0. 25065(17) nm, which are in the range of other six-coordinate analogues, $\text{Ni}[\text{S}_2\text{P}(\text{OCH}_2\text{CH}_2\text{Ph})_2 \cdot \text{bipy}]^{[17]}$ (0. 2488 (5) to 0. 2513 (5) nm), $\text{Ni}[\text{S}_2\text{P}(\text{OC}_6\text{H}_4\text{M}-\text{e}-\text{p})]_2 \cdot \text{bipy}^{[19]}$ (0. 24757(7) to 0. 25096(6) nm), $\text{Ni}[\text{S}_2\text{P}(\text{OC}_6\text{H}_4\text{M}-\text{e}-\text{p})]_2 \cdot \text{phen}^{[20]}$ (0. 2486(1) to

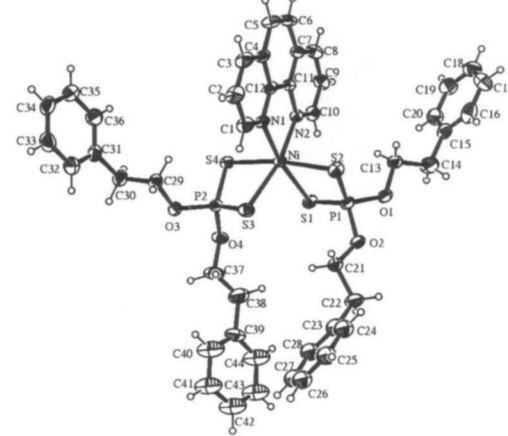


Figure 1 Perspective view of adduct 1 showing 30% probability thermal ellipsoids

0. 2532(1) nm) and $\text{Ni}[\text{S}_2\text{P}(\text{OMe})_2] \cdot \text{phen}^{[14]}$ (0. 247 (1) to 0. 252(1) nm). And the $\text{Ni}-\text{S}$ distances in adduct **1** are much longer than those in the square planar four-coordinate $\text{Ni}[\text{S}_2\text{P}(\text{OCH}_2\text{CH}_2\text{Ph})_2]_2$ (0. 22202 (11) and 0. 22228(13) nm)^[22], resulting from the change of coordination-geometry and the increase in steric hindrance. The $\text{Ni}-\text{N}$ distances are fairly similar in adduct **1** (0. 2081(3) and 0. 2090(5) nm) which is also in good agreement with the bond lengths found in these six-coordinate $\text{Ni}[\text{S}_2\text{P}(\text{OMe})_2] \cdot \text{phen}^{[14]}$ (0. 208 (1) to 0. 209 (1) nm), $\text{Ni}[\text{S}_2\text{P}(\text{OCH}_2\text{CH}_2\text{Ph})_2 \cdot \text{bipy}]^{[17]}$ (0. 2072(13) to 0. 2086 (13) nm), $\text{Ni}[\text{S}_2\text{P}(\text{OC}_6\text{H}_4\text{M}-\text{o}-\text{o})]_2 \cdot \text{bipy}^{[19]}$ (0. 2060 (1) to 0. 2079 (1) nm), $\text{Ni}[\text{S}_2\text{P}(\text{OC}_6\text{H}_4\text{M}-\text{e}-\text{p})]_2 \cdot \text{phen}^{[20]}$ (0. 2082(3) to 0. 2086(3) nm). The average distances of the four $\text{P}-\text{S}$ bonds (0. 1975(2) nm) in adduct **1** is shorter than that in $\text{Ni}[\text{S}_2\text{P}(\text{OCH}_2\text{CH}_2\text{Ph})_2]_2^{[22]}$ (0. 19889(15) nm), which shows that the increase in steric hindrance has no significant influence on the partial double bond character of these $\text{P}-\text{S}$ bonds. All other bond distances are normal.

The $\text{N}1-\text{N}2$, $\text{S}1-\text{N}2$ and $\text{S}3-\text{N}2$ bite angles in adduct **1** are similar to the values found previously in the six-coordinate adducts $\text{Ni}[\text{S}_2\text{P}(\text{OCH}_2\text{CH}_2\text{Ph})_2 \cdot \text{bipy}]^{[17]}$, $\text{Ni}[\text{S}_2\text{P}(\text{OC}_6\text{H}_4\text{M}-\text{e}-\text{o})]_2 \cdot \text{bipy}^{[19]}$, $\text{Ni}[\text{S}_2\text{P}(\text{OC}_6\text{H}_4\text{M}-\text{e}-\text{p})]_2 \cdot \text{phen}^{[20]}$, and $\text{Ni}[\text{S}_2\text{P}(\text{OMe})_2] \cdot \text{phen}^{[14]}$, which are 79. 69(16), 81. 27(5) and 81. 36(5)°, respectively. The small bite angles of the phen and O, O' -di(2-phenyl ethyl) dithiophosphate ligands result in very acute bond angles for an octahedral geometry. This distortion is also reflected in the bond angles between the *trans* ligands. The $\text{S}2-\text{N}2-\text{S}4$

bond angle is $170.94(5)^\circ$ compared to $170.23(12)^\circ$ and $167.39(12)^\circ$ for the N1-N1S1 and N2-N2S3 bond angles. The deviation of these angles from idealized octahedral geometry is also due to the fact that two four-member chelating rings occur for the chelating O, O'-di(2-phenyl ethyl)dithiophosphates while phen forms five-member chelating ring. Therefore, small bite angles for phen and O, O'-di(2-phenyl ethyl)dithiophosphate ligands as well as four- and five-member chelating rings lead to a very distorted octahedron for adduct **1**.

The phen ligand and the nickel atom of adduct **1** lie approximately in one plane. Atom C2 shows a maximum deviation of 0.0075 nm from the least-squares chelating plane. The atom P1 has a maximum deviation of 0.0013 nm from the least-squares chelating plane defined by atoms N1, S1, P1, and S2. The largest deviation from the least-squares chelating plane of N1, S3, P2, and S4 is 0.0128 nm for P2 much larger than that of P1 (0.00013 nm).

Interestingly, weak π - π stacking and hydrogen bond interactions are found in the crystal structure. There exist weak intermolecular C3H...S1ⁱ hydrogen-bonding interactions [symmetry code (i): $-1+x, y, z$] between molecules having the same configuration, with distance of $0.3761(7)\text{ nm}$, which is shorter than that in complex $[\text{Mn}(\text{NCS})_2(\text{Eim})_4]$ (0.3856 nm , where Eim is 1-ethylimidazole)^[25]. The C3H...S1ⁱ hydrogen-bonding interactions link the molecules into a 1D chain along the a -axis as showed in Fig. 2. And inter-chain face-to-face π - π stacking interactions occur between aromatic rings of phen ligands in the adjacent 1D chains C4~C7/C11~C12 and C4ⁱⁱ~C7ⁱⁱ/C11ⁱⁱ~C12ⁱⁱ [symmetry code (ii) $1+x, y, z$], with dihedral angles of 0.00° and inter-planar distance of $0.3604(2)\text{ nm}$, centroid-to-centroid distance of $0.3652(4)\text{ nm}$, and slippage distance of $0.0594(3)\text{ nm}$. The inter-planar distance is shorter than that in complex Cu(phth)₂(H₂O)^[26] (0.3647 nm) and $[\text{Co}(p\text{-ClC}_6\text{H}_4\text{CO}_2)_2(\text{phen})(\text{H}_2\text{O})_2]$ ^[27] (0.3684 nm), meanwhile, the centroid separation is shorter than that of $[\text{Zn}(\text{H}_2\text{O})_6](\text{HL})$ ^[28] (0.3672 nm , H₂L is 1-(4-hydroxyphenyl)-5-thioacetatetrazole). Thus a 1D chain-pair structure unit along the a -axis is assembled through the inter-chain π - π stacking interactions and weak inter-chain C9H...O4ⁱⁱⁱ hydrogen-bonding interactions [symmetry code (iii): $2-x, -y, -z$ with distance of $0.3415(7)\text{ nm}$] (Fig.

2). An interesting feature of the 1D chain-pair resides in that all molecules constructing a 1D chain have the same configuration and molecules in the adjacent different 1D chain have the opposite configuration.

Table 3 Hydrogen bonds length (nm) and bonds angle (°) for adduct 1

D-H...A	d(D-H)/nm	d(H...A)/nm	d(D...A)/nm	\angle (DHA)/(°)
C3H...S1 ⁱ	0.093	0.2868	0.3761(7)	162.74(3)
C9H...O4 ⁱⁱⁱ	0.093	0.2481	0.3415(7)	177.56(2)
C34H...S2 ^{iv}	0.093	0.2958	0.3476(6)	143.47(3)
C30H30A...O2 ^v	0.097	0.2593	0.3469(8)	152.23(6)

* Symmetry transformations used to generate the equivalent atoms: i $-1+x, y, z$; ii $2-x, -y, -z$; iii $4-1-x, -1/2+y, 1/2-z$; iv $2-x, -1/2+y, 1/2-z$.

The most striking structural feature of adduct **1** is that it forms 1D helical chain structure through potentially weak intermolecular C34H...S2^{iv} hydrogen-bonding interactions [symmetry code (iv): $1-x, -1/2+y, 1/2-z$ with distance of $0.3476(6)\text{ nm}$] (Fig. 3(A))^[29-31]. Obviously, the hydrogen bonds undoubtedly steer the rotation direction of the helix. The adduct **1** is uniformly spaced column along the b -axis. The nearest N...N distance within the columns is 2.1432 nm , and the repeating period in the helical chain is identical with the former. In addition, unlike the most double-helical complexes^[32-37], the adjacent helical chains in adduct **1**, one exhibiting left-handedness and the other right-handedness, are not entangled together but hydrogen bonding which are alternatively offered by two helical chains to generate a 1D double-stranded helical chain as showed in Fig. 3(A). To illustrate this clearly, the left- and right-handed helical chains are represented respectively in Fig. 3(B), 3(C). Because left-handed and right-handed helical chains coexist in the crystal structure, the whole crystal is mesmeric and does not exhibit chirality^[38].

Furthermore, the another inter-chain C30H30A...O2^v hydrogen-bonding interactions [symmetry code (v): $2-x, -1/2+y, 1/2-z$ with distance of $0.3469(8)\text{ nm}$] link the 1D chain-pair and the double-stranded helical chain into a 3D supramolecular network.

2.2 IR and UV-vis Spectra Studies

The IR spectrum of the nitrogen base adduct **1** shows two strong intensity bands present at 1057 and 996 cm^{-1} are assigned to $\nu[(\text{P}-\text{O}-\text{C})]$ stretching vibrations while a strong band at 868 cm^{-1} is assigned to $\nu[\text{P}-\text{O}-(\text{C})]$ stretching vibration. Two strong bands due to PS₂ asymmetric and symmetric stretching vibrations in the adduct are observed at 670 and 601 cm^{-1} , respectively^[17, 19]. The weak band at 3027 cm^{-1} may be

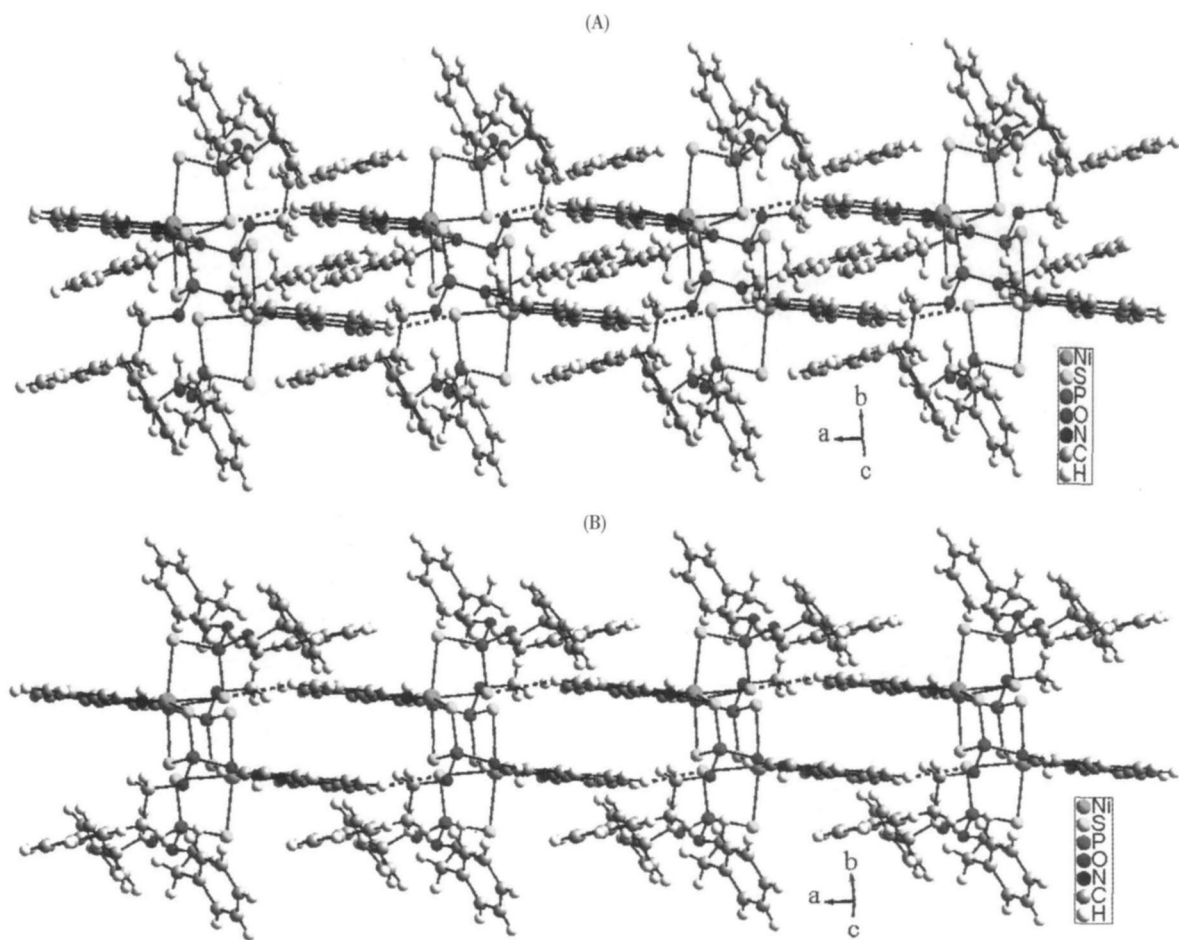


Figure 2 1D chain-pair structure consist from $\pi\cdots\pi$ stacking $C_3\text{-H}\cdots S^{i\prime}$ interactions and $C_9\text{-H}\cdots O_4^{ii\prime}$ interactions (A), dotted line indicating the hydrogen bonds (B) with part of phenylethyl groups omitted for clear

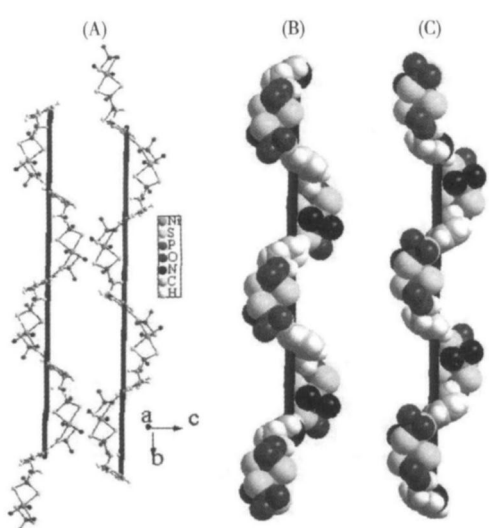


Figure 3 (A) 1D double-stranded helical chain formed by $C_{34}\text{-H}\cdots S^{i\prime\prime}$ hydrogen-bonding interactions (B) left handed and (C) right handed (phen ligands and part of phenylethyl groups omitted for clarity)

assigned to the unsaturated C-H bond stretching vibrations of the phenyl group and 1, 10-phenanthroline ligand. The bands at 1604, 1494, 1453 and 1422 cm^{-1} may be attributed to the skeleton vibrations of the phenyl group and 1, 10-phenanthroline ligand, but the bond at 1626 cm^{-1} due to $\nu(\text{C}=\text{N})$ stretching vibration of phen ligand^[15].

The UV-vis spectrum of the adduct **1** in CHCl_3 is shown in Fig. 4. The adduct shows an absorption band at 268 nm that can be attributed to ligand absorption band and /or ligand-to-metal charge transfer band (LMCT). As expected for high-spin octahedral Ni(II) complex, spin allowed $d\text{-}d$ bands are observed at 661 and 1122 nm that are assigned to the $^3\text{A}_{2g}\rightarrow ^3\text{T}_{1g}$ (F) and $^3\text{A}_{2g}\rightarrow ^3\text{T}_{2g}$ (F) transition, respectively. A weak band at 900 nm is due to the spin-forbidden $^3\text{A}_{2g}\rightarrow ^3\text{E}_{1g}$ transition. The bands at 382 and 414 nm are attributed to the third d-d ($^3\text{A}_{2g}\rightarrow ^3\text{T}_{1g}$ (P)) for d^8 octahedral Ni(II) complex^[19, 39].

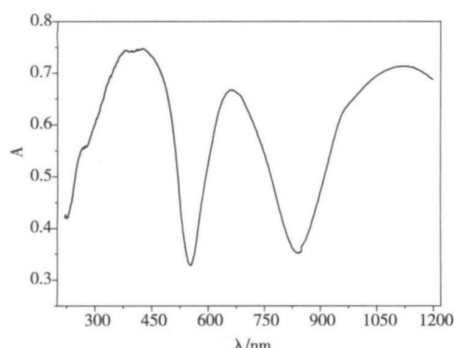


Figure 4 Ultraviolet-visible spectroscopy of adduct 1

2.3 Thermal Analysis

Fig 5 indicates the TG-DSC curves at atmosphere from 35°C to 700°C. The adduct **1** has a sharp endothermic peak and has no weight loss at 152.3°C, which is attributed to heat-absorbing of adduct **1** melting. The adduct **1** begins to loss weight at 179.0–279.0°C corresponding to two 2-phenylethyl-oxy groups (anal 25.46%, calc 26.52%), which is assigned to the second weak broad endothermic peak at 206.7°C. Then the weight loss of 18.22% for the adduct **1** at 297.0–422.0°C corresponding to **1**, 10-phenanthroline ligand (calc 17.09%), which is assigned to the first exothermic peak at 379.4°C and the third endothermic peak at 387.9°C. And last the continuous weight loss for adduct **1** is observed above 422.0°C corresponding to removing the residual organic ligands continuously and there isn't thermoeffect any more at DSC curve.

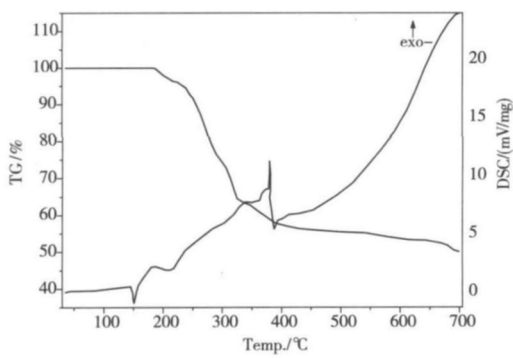


Figure 5 TG-DSC curves of adduct 1

3 Conclusions

A nitrogen base adduct **1**, 10-phenanthroline bis(O, O'-di(2-phenylethyl)dithiophosphato) nickel(II), Ni[S₂P(OCH₂CH₂Ph)₂]₂ · phen(I) has been synthesized. X-ray crystallography shows that adduct **1** consist of 1D chain-pair and 1D double-stranded helical chain, which formed

from π-π stacking of phen ligands and hydrogen-bonding interactions of C-H...S and C-H...O. They are further extended to 3D supramolecular network by C-H...S hydrogen-bonding interactions.

Note

Crystallographic data excluding structure factors for the structural analysis has been deposited with the Cambridge Crystallographic Data Center as supplementary publication No 774426 for adduct **1**. Copies of the data can be obtained free of charge via <http://www.ccdc.cam.ac.uk/deposit.html> (or from The Director, CCDC, 12 Union Road, Cambridge CB2 1EZ, UK, by Fax 0044-1223-336-033 or Email deposit@ccdc.cam.ac.uk).

References

- [1] Masuko M, Sato H, Suzuki A, et al Prevention of oxidative degradation of ZnDTP by microencapsulation and verification of its antioxidant performance [J]. Tribology International 2008, 41(11): 1097-1102
- [2] Hu J Q, Wei X Y, Dai G L, et al Tribological behaviors and mechanism of sulfur and phosphorus-free organic molybdate ester with zinc dialkyl dithiophosphate [J]. Tribology International 2008, 41(6): 549-555
- [3] Larsson A C, Ivanov A V, Antzutkin O N, et al Complexation of lead(II) with O, O'-dialkylthiophosphate ligands ³¹P and ¹³C CP/MAS NMR and single-crystal X-ray diffraction studies [J]. Inorg Chim Acta 2004, 357: 2510-2518
- [4] Ivanov M A, Antzutkin O N, Shanutin V V, et al. Preparation and structural organization of heteroleptic tetraphenyltin(IV) complexes comprising unidentately and bidentately coordinated O, O'-dialkyl dithiophosphate groups. Multinuclear(³¹C, ³¹P) CP MAS NMR and single-crystal X-ray diffraction studies [J]. Inorg Chim Acta 2007, 360: 2897-2904
- [5] Maheshwari S, Drake JE, Kori K M, et al Synthesis and spectroscopic characterization of tris(O, O'-ditolylthiophosphato) arsenic/antimony bisimides (III) compounds. Crystal structures of [As{S₂P(OC₆H₄Mes)₂}₃]⁺ · 0.5C₆H₁₄, [Sb{S₂P(OC₆H₄Mes)₂}₃]⁺ and [Bi{S₂P(OC₆H₄Mes)₂}₃]⁺ [J]. Polyhedron 2009, 28(4): 689-694
- [6] Liu C W, Liu M D, Mohan A A, et al. Cluster self-assembly of centered cubes of copper(I) with dialkyl ligands X-ray structures of Cu₈(DDP)₆(μ₈-X)₂PF₆ (DDP = S₂P(O'_{Pr})₂; X = Cl or Br) and their relationship to oxide and sulfide centered zinc(II) dialkyl thiophosphates [Zn₄(DDP)₆(μ₄-S or O)] [J]. Inorg. Chim. Acta 2004, 357: 3950-3956
- [7] Menzer S, Phillips J R, Shaw A M Z, et al Structural characterization of basic zinc O, O'-dialkylthiophosphosphate and two iso-

- meric examples of zinc monothiophosphates [J]. *J Chem Soc, Dalton Trans*, 2000(19): 3269-3273
- [8] Matsumoto K, Tanaka R, Shimomura R, et al. Synthesis and X-ray structures of octanuclear silver(I) cluster [$\text{Ag}_8(\mu_6\text{-S})\{\text{S}_2\text{P}(\text{OC}_2\text{H}_5)_2\}_6$] and its copper(I) analogue [$\text{Cu}_8(\mu_8\text{-S})\{\text{S}_2\text{P}(\text{OC}_2\text{H}_5)_2\}_6$] [J]. *Inorg Chim Acta*, 2000, 304: 293-296
- [9] Drew M G B, Hasan M, Hobson R J, et al. Reaction of [$\text{Zn}\{\text{S}_2\text{P}(\text{O}\text{-Pr})_2\}_2 \cdot \text{H}_2\text{NCH}_2\text{CH}_2\text{NH}_2$] and [$\text{Zn}\{\text{S}_2\text{P}(\text{O}\text{-Pr})_2\}_2 \cdot \text{NC}_5\text{H}_5$] [J]. *J Chem Soc, Dalton Trans*, 1986(6): 1161-1166
- [10] Harrison P G, Begley M J, Kabhai T, et al. Zinc(II) bis(O,O'-diethylthiophosphates): complexation behavior with pyridine and other multidentate nitrogen donor molecules. The crystal and molecular structures of the 1:1 complexes of bis(O,O'-diisopropylthiophosphato) zinc(II) with pyridine, 2,2'-bipyridine, and 2,2':2''terpyridine and of (1,11-diamino-3,6,9-triazaundecane) zinc(II) bis(O,O'-diethylthiophosphate) [J]. *J Chem Soc, Dalton Trans*, 1986(5): 929-938
- [11] Harrison P G, Begley M J, Kabhai T, et al. Complexes of lead(II) bis(O,O'-diethylthiophosphates) with nitrogen donor ligands. The crystal structures of $\text{Pb}[\text{S}_2\text{P}(\text{OEt})_2] \cdot \text{en}$ (en = ethylenediamine), $\text{Pb}[\text{S}_2\text{P}(\text{OEt})_2] \cdot \text{bipy}$ (bipy = 2,2'-bipyridine) and $\{\text{Pb}[\text{S}_2\text{P}(\text{OEt})_2]_2\} \cdot \text{en}$ [J]. *J Chem Soc, Dalton Trans*, 1989(12): 2443-2448
- [12] Drew M G B, Forsyth G A, Hasan M, et al. Reactions of copper(II) with $[\text{S}_2\text{P}(\text{OR})_2]$ (R = Et or Prⁱ) and single crystal X-ray studies of $\text{Cu}[\text{S}_2\text{P}(\text{OEt})_2] \cdot \text{bipy}$ and $\text{Cu}[\text{S}_2\text{P}(\text{OEt})_2] \cdot 2\text{PPh}_3$ [J]. *J Chem Soc, Dalton Trans*, 1987(5): 1027-1033
- [13] Li Z H, Li J R, Du S W. Construction of three novel luminescent polymers containing $\{\text{Cu}_2\text{S}_2\text{P}(\text{OR})_2\}$ (R = Me, Et) building blocks linked by 4,4'-bipyridine ligands [J]. *J Mol Struct*, 2006, 783(6): 116-121.
- [14] Shetty P S, Fernando Q. Structures of five and six coordinated mixed ligand chelates of nickel(II) containing sulfur and nitrogen donor atoms [J]. *J Am Chem Soc*, 1970, 92(13): 964-969.
- [15] 刘世雄, 林墀昌, 徐正, 等. 双-(O,O'-二正基二硫代磷酸酯)合镍-2吡啶加合物的晶体结构和分子结构 [J]. 有机化学, 1987, 7(5): 369-373
- [16] 游效曾, 徐正, 徐昕, 等. 双-(O,O'-二环己基二硫代磷酸酯)合镍(II)与苯胺的加合常数及加合物 $\text{Ni}[(\text{C}_6\text{H}_{11}\text{O})_2\text{PS}_2]_2 \cdot 2\text{NH}_2\text{CH}_2\text{C}_6\text{H}_5$ 的晶体结构 [J]. 化学通报, 1991, 36(17): 1308-1311
- [17] 谢斌, 程煜, 邹立科, 等. 三元配合物 $\text{Ni}[\text{S}_2\text{P}(\text{OCH}_2\text{CH}_2\text{Ph})_2]_2 \cdot \text{bipy}$ 的合成与晶体结构 [J]. 化学通报, 2009, 72(1): 70-74
- [18] Zou L K, Xie B, Zhao B, et al. Bis(2-henyl) di-thiophosphato bipyridine nickel(II) [J]. *Acta Cryst*, 2006, 62: 2830-2830
- [19] Bingham A L, Drake J E, Hirsthouse M B, et al. Synthesis, characterization and spectral studies of nitrogen base adducts of bis(O,O'-diethylthiophosphato) nickel(II). Crystal structures of $\text{Ni}[\text{S}_2\text{P}(\text{OC}_6\text{H}_4\text{MePr})_2]_2 \cdot \text{C}_{10}\text{H}_8\text{N}_2$ and $\text{Ni}[\text{S}_2\text{P}(\text{OC}_6\text{H}_4\text{MePr})_2]_2 \cdot \text{H}_2\text{NCH}_2\text{CH}_2\text{NH}_2$ [J]. *Polyhedron*, 2007, 26(12): 2672-2678
- [20] Hao Q, Fan H K, Chantapromma S, et al. Bis(O,O'-diethylthiophosphato) nickel(II) [J]. *Acta Cryst*, 2001, 57: 717
- [21] 谢斌, 李可彬, 邹立科, 等. 含四氮杂大环的双(O,O'-二(2-苯乙基)二硫代磷酸根)合镍(II)或铜(II)配合物的合成和晶体结构 [J]. 结构化学, 2004(23): 324-331
- [22] Zou L K, Xie B, Xie J Q, et al. Kinetic study of the hydrolysis of a carboxylic acid ester promoted by the complex bis(O,O'-di(2-phenylethyl) di-thiophosphato) nickel(II) [J]. *Transition Met Chem*, 2009, 4(4): 395-401
- [23] Shekllirk G M. SHELXTL, Structure determination software program Version 5.10. Bruker analytical X-ray systems [M]. Inc Madison WI 1997.
- [24] Franscina L J W in GX suite for small molecule single crystal crystallography [J]. *J Appl Cryst*, 1999, 32: 837
- [25] 刘法谦, 李荣勋, 李少香. 四(1乙基咪唑)二异硫氰酸锰的晶体结构和热性能 [J]. 无机化学学报, 2008, 24(1): 141
- [26] 武文, 谢吉民. 之字链配合物 $\text{Cu}(\text{phH})_2(\text{H}_2\text{O})_2$ 的合成、表征及晶体结构 [J]. 人工晶体学报, 2008, 37(5): 1172-1176
- [27] 金晶, 刘佳操, 赵力民, 等. Co(II)配位超分子的水热合成、晶体结构及光物理性能 [J]. 辽宁师范大学学报: 自然科学版, 2008, 31(4): 478-481
- [28] 张曙光, 冯云龙, 温一航. H键连接的三维超分子化合物 [M] (H_2O_6) (HL)₂ 的合成、表征与结构 [$\text{H}_2\text{L} = 1\text{-}(4\text{-羟基苯})-5\text{-四氮唑乙酸}$, $\text{M} = \text{Mn}^{II}, \text{Co}^{II}, \text{Ni}^{II}, \text{Zn}^{II}$] [J]. 无机化学学报, 2008, 24(4): 581-585
- [29] Glauert J P, Lewis M, Rossi M. Crystal structure analysis for chemists and biologists [M], New York: VCH Publishers Inc, 1994
- [30] Steiner T. C-H...O Hydrogen bonding in crystals [J]. *Cryst Log Rev*, 1996, 6(1): 1-51.
- [31] Hunter R H, Hausein R H, Irving A. The first water-dependent liquid clathrate X-ray evidence in the solid for a C-H...π (heteroarene)...H-C interaction [J]. *Angew. Chem, Int Ed Engl*, 1994, 33(5): 566-568
- [32] Lu C Z, Wu C D, Lu S F, et al. A three-dimensional zeolite-like organic-inorganic hybrid material constructed from $\{\text{CuM}_2\text{O}_8\text{N}\}_n$ double helical chains linked via $[\text{Cu}(4,4'\text{-bpy})]_n$ fragments [J]. *Chem Commun*, 2002(2): 152-153
- [33] Wang Y, Yu J H, Guo M, et al. $[\{\text{Zn}(\text{HPO}_4)_4\} \cdot \{\text{Co}(\text{dien})_2\}] \text{H}_3\text{O}$: A zinc phosphate with multidirectional intersecting helical channels [J]. *Angew. Chem, Int Ed Engl*, 2003, 42(34): 4089-4092
- [34] Qin C, Wang X L, Li Y G, et al. Three-dimensional mesmeric networks assembled from helix-linked sheets syntheses structures, and magnetisms [J]. *J Chem Soc, Dalton Trans*, 2005(15): 2609-2614
- [35] Wu Z, Chen Q, Xiong S, et al. Double-stranded helicates triangles and squares formed by the self-assembly of pyrrolidine-2-yl methyle Publishing House. All rights reserved. <http://www.cnki.net>

- neanines and Zn^{II} ions[J]. Angew. Chem. Int Ed, 2003, 42(28): 3271-3274
- [36] Barboiu M, Vaughan G, Graff R, et al Self assembly structure and dynamic interconversion of metallo-supramolecular architectures generated by Pb(II)-binding induced unfolding of a helical ligand[J]. J Am. Chem. Soc., 2003, 125(34): 10257-10265
- [37] Wang X L, Qin C, Wang E B An unusual polyoxometalate-encapsulating 3D polyrotaxane framework formed by molecular squares threading on a two-fold interpenetrated diamondoid skeleton[J]. J. Mater. Chem., 2007, 41: 4245-4247
- [38] Wang X L, Qin C, Wang E B, et al Syntheses structures and photoluminescence of a novel class of d¹⁰ metal complexes constructed from pyridine-3,4-dicarboxylic acid with different coordination architectures[J]. Inorg. Chem., 2004, 43(6): 1850-1856
- [39] Holz R C, Evdokimov E A, Gobena F T Two-dimensional ¹H NMR studies on octahedral nickel(II) complexes[J]. Inorg. Chem., 1996, 35(13): 3808-3814

1, 10-林菲啰啉·双(O, O'-二(2-苯乙基)二硫代磷酸)合镍(II)的合成与晶体结构

谢斌^{1,2}, 邹立科^{1,2}, 赖川³, 黄春³, 王军^{1,2}, 相阳光³

(1. 四川理工学院功能材料研究所, 四川 自贡 643000; 2. 绿色催化四川省高校重点实验室, 四川 自贡 643000;
3. 四川理工学院材料与化学工程学院, 四川 自贡 643000)

摘要: 在石油醚和丙酮溶液中, 配合物 Ni[S₂P(OCH₂CH₂PH)₂]₂与1, 10-邻菲啰啉(phén)反应得到了绿色的氮碱加合物1, 10-林菲啰啉·双(O, O'-二(2-苯乙基)二硫代磷酸)合镍(II), 用元素分析、紫外-可见光谱、红外光谱、热分析和X射线单晶衍射进行了表征。加合物属单斜晶系, P2₁/c空间群。晶胞参数为a = 1.0987(9) nm, b = 2.1432(9) nm, c = 1.9025(5) nm, β = 98.68(1)°, V = 4.429(4) nm³, Z = 4, D_c = 1.370 M g/m³, F(000) = 1904, μ = 0.743 mm⁻¹, 可观测衍射点为3498, R = 0.057, wR = 0.1492(I(20(I))). 加合物为畸变八面体构型, 配位原子来自于两个O, O'-二(2-苯乙基)二硫代磷酸根的4个硫原子和配体phen的2个氮原子。Ni-S键的键长在0.2474(2)-0.2505(17) nm范围内, Ni-N键的键长分别为0.2081(4) nm和0.2090(5) nm。因分子间存在π-π堆积、C-H...O和C-H...S氢键作用, 加合物的晶体结构形成了一维链对和一维双链螺旋链。一维链对和一维双链螺旋链通过C-H...O氢键作用进一步延展为三维结构。

关键词: O, O'-二烃基二硫代磷酸; 镍(II)加合物; 合成; 表征; 晶体结构